

# **Weak-Antilocalization induced Enhanced Surface Conductivity and topological protection in Topological Insulator Thin films**

R.K. Gopal, Sourabh Singh, Arpita Mandal, Jit Sarkar, Sandeep Tammu, Partha Mitra, Chiranjib Mitra

Indian Institute of Science Education & Research Kolkata, Mohanpur - 741246, India

## **Abstract:**

We report magnetotransport measurements on ternary tetradymite Topological Insulating compound  $\text{Bi}_2\text{Se}_2\text{Te}$  thin films deposited by pulsed laser deposition technique. The temperature dependent resistance of these thin films shows insulating ground state followed by insulator to surface metallic transition at low temperature. Hence we anticipate that the chemical potential of these thin films lie in the bulk insulating gap, a fundamental requirement of topological insulating materials for the device applications. Such a bulk insulating state is known as the topological transport regime as shown by temperature dependence of resistance. Manifestation of topological protection and surface dominated transport has been elaborately explained by weak antilocalization data and low temperature (less than 50K) down turn in resistance of these thin films. The Magnetoresistance of these thin films exhibit pronounced weak antilocalization behavior with a sharp cusp in the vicinity of zero magnetic field. Surface states have been found remarkably robust even at reasonably high temperatures (100K) exhibiting linear MR in high field regime in agreement with other reports. Our findings are crucial for the understanding of transport behavior of TI's and pave the way towards realizing novel device applications.

## **Introduction:**

Presence of an odd number of helical Dirac cones on the surface and a  $\pi$  Berry phase have made Topological insulators (TI) a promising class of materials that exhibit numerous exotic phenomena such as topological delocalization towards time reversal invariant (non-magnetic) impurities and defects<sup>123</sup>. The linear dispersion of these surface Dirac states along with helical spin texture make them distinct from other trivial two dimensional surface states (2DEG) or other strongly spin orbit coupled (SOC) systems. These spin filtered Dirac states are robust to any amount of non-magnetic disorder, interactions and defects which is in stark contrast to the trivial 2DEG systems and SOC systems, which become localized when subjected to the disorder<sup>45</sup>. This nontrivial phase of insulators have been characterized by a  $Z_2$  topological quantum number which makes this phase distinct from conventional insulators with bulk gap:  $Z_2=-1$  and 0 for TI (2D, while four  $Z_2$  invariants for the classification in 3D TIs )and trivial insulators respectively<sup>6</sup>. This topological classification ensures that smooth deformations in the system will not change the physical properties of the TI, but cannot be deformed in to a trivial insulator unless the gap closes. The topological order of the bulk wave function is responsible for such nontrivial states appearing on

the surface of a TI as odd number of Dirac cones. This  $Z_2$  topologically ordered state guarantees presence of odd number of Fermi surface owing to formation of Kramer's doublet and decides the number of surface modes (edge modes in 2D) which cannot be gapped by tuning the disorder (chemical potential)<sup>1,7</sup>. This type of even/odd topological effects is manifested in the magnetotransport, surface sensitive probes and magneto-optical experiments<sup>8,9,10,11-13</sup>. It is this  $Z_2$  quantum number, (even –odd number of Dirac cones) which separates TI's fundamentally from graphene and other trivial 2D electron systems.

There are a number of evidences on surface dominated transport on thin films and nano-devices, exhibiting two dimensional nature of quantum interference phenomena like two dimensional weak antilocalization(WAL), Shubnikov de – Hass (SdH) oscillations and Aharonov – Bohm(AB)Oscillations in magnetoresistance measurement experiments<sup>8,9,14-16</sup>. These experiments provide direct evidence of quantum mechanical nature of these robust surface Dirac states exhibiting two dimensional (2D) quantum interference while encountering an impurity on their way<sup>17,18</sup>. Impurities and defects act like an obstacle or slit to ordinary waves. Their intensity pattern depends on the relative phase between the two paths, which is also true in case of Dirac states having shown unequivocally a Berry phase of  $\pi$  in MR oscillations mentioned above<sup>9,12,14,16</sup>. The device application of TI's in terms of spintronics is not far away since some of remarkable applications are already underway on the basis of recent results<sup>19-21</sup>.

In the past few years there has been an intense search for better topological insulators than the earlier binary alloys  $\text{Bi}_2\text{Te}_3$  (BT),  $\text{Bi}_2\text{Se}_3$  (BS) and  $\text{Sb}_2\text{Te}_3$  (ST). That is because these alloys have finite residual bulk contribution to transport as it is evident from transport experiments, which in turn masks the surface transport signals. These alloys are not in the so called topological transport regime. In topological transport regime the Fermi level lies in the bulk gap, thus making the bulk insulating and conduction is dominated by the surface electrons arising out of the Dirac like surface states<sup>22-26</sup>. The defects and vacancies in these materials derive the chemical potential in to the conduction band making them effectively metallic in nature and it is manifested in the temperature dependent resistivity behavior of these thin films and devices. This has been well established by surface sensitive probes such as angle resolved photoemission experiments and scanning tunneling spectroscopy/microscopy on binary and ternary TI materials<sup>1,27,28</sup>. Significant efforts have been devoted to suppress these defect induced bulk conduction which include compensation doping (Sn, Cd, Sb, etc.) and electrostatic tuning of the Fermi level. But still there are contributions from the metallic bulk and the doping further aggravates the situation by introducing structural defects<sup>29</sup>. Therefore these extrinsic TI's do not seem to be promising candidates. Ternary and quaternary topological insulators materials,  $\text{Bi}_2\text{Se}_2\text{Te}$  (BST),  $\text{Bi}_2\text{Te}_2\text{Se}$  (BTS),  $\text{Bi}_{2-x}\text{Sb}_x\text{Te}_3$ ,  $\text{Bi}_{2-x}\text{Sb}_{1-x}\text{Se}_3$  and  $\text{Bi}_x\text{Sb}_{1-x}\text{Te}_y\text{Se}_{1-y}$  (BSTS), on the other hand seem to be having the Fermi level inside the band gap<sup>9,14,21,28,30</sup>. ARPES measurement validates the above point and hence these ternary tetradymites fulfill the criteria of intrinsic topological insulators. Thus these materials are ideal and promising candidates for realizing surface dominated transport leading to fabrication of spintronic devices harnessing surface Dirac electrons<sup>19,20</sup>. BTS has been well established as a better topological insulator by means of several transport and spectroscopic studies performed on it (showing bulk resistivity as high as 6 ohm.cm at 4K), but less attention has been paid on BST

which is considered to be a better candidate in terms of spin texture and lesser hexagonal warping of the Dirac cone<sup>9,16,23,31–33</sup>

In the case of BST the Dirac point is located nearly in the center of the band gap, while for BTS it is embedded downwards in the bulk valence band. This location of the Dirac point for BST and BTS is due to the derivation of these compounds from parent materials, BS and BT respectively<sup>16,23,28,34,35</sup>. It is therefore interesting to note here that although BTS has high resistivity, but to observe various exotic phenomena such as topological magneto-electric effect by opening gap in the surface Dirac states, BST is much more promising owing to its unique positioning of the isolated Dirac point nearly in the middle of bulk band gap. Currently the focus has been shifted towards these materials in terms of compositional and band structure engineering owing to their superiority over binary alloys<sup>30,35,36</sup>.

Moreover, it has been experimentally verified that the shape of the Dirac cone and position of the Dirac point changes with the proper compositional engineering<sup>35</sup>. Previously Dirac dispersion in binary TI's was found to be little nonlinear and warped away from the Dirac point, which led to the development of out of plane spin component on the Dirac cone, reducing complete suppression of the backscattering<sup>33,37,38</sup>. Tuning of these band structure parameters has profound effect on the surface electronic dominated transport and optical properties: Fermi velocity of Dirac states (slope of Dirac cone) increases and it is easy to manipulate surface states in the bulk gap (Ambipolar surface conduction)<sup>35,36</sup>. The transport signature of the surface Dirac states have been achieved unambiguously with very less or no parasitic bulk effects in such ternary and quaternary TI devices/single crystals. Recent spin sensitive experiments performed on these material devices have clearly demonstrated Dirac states dominated features up to remarkable high temperatures<sup>20,39</sup>

Another advantage of these ternary materials in comparison to binary ones is the presence of topological surface states below Dirac point with high degree of spin texture (reduced hexagonal warping), which was found to be buried in the bulk valence bands in the latter case<sup>16,23,35,36</sup>. Therefore for the device storage and spintronics applications both Dirac cones could be accessed easily. These observations have been revealed in spin resolved photoemission experiments, justifying unambiguously the topological nature of surface states well below Dirac point. Moreover, their experimental observation clearly shows better Dirac cone structure in terms of hexagonal warping, spin polarizability and position of Dirac cone itself in the bulk gap. These properties of materials with high bulk insulating character have certainly paved the way for spintronics and other device applications<sup>19,20,40–42</sup>.

### **Experimental:**

BST thin films were grown on Si (001) substrates at different temperatures (250°C- 350°C)<sup>31</sup>. Substrate heating is an important parameter for epitaxial and ordered growth of thin films. The composition and quality of the film is affected by the reaction kinetics and the reaction rate of the reactant species. The substrate temperature controls both the reaction rate and its kinetics. We observed that samples prepared in 250°C – 300°C were better in comparison to the ones grown on high substrate temperature in terms of morphology, grain size and crystal structure<sup>43,44</sup>. The substrates were cleaned by immersing them in 5% HF solution for 10 minutes followed by

ultrasound bath for 15 minutes in DI water. Prior to growth substrates were degassed at elevated temperature of 400°C and subsequently flushed by inert gas (Argon) twice to get rid of impurities and oxide contaminations on the surface. Substrates were then cooled slowly to the deposition temperature. The ablation target material for BST thin films was prepared by grinding BS and BT materials in a stoichiometric ratio of 2:1 to get exact BST composition of thin films. The finely ground resultant material was pressed to form a pellet and subsequently it was then annealed at 400°C for 4hr in an inert (Argon) atmosphere followed by cooling it slowly for 4hrs.

Thin films of thicknesses nearly 300nm to 500nm were deposited at low repetition rate of 1Hz and at a laser fluence of 1.5J/cm<sup>2</sup>. All the results reported in this work are of 300nm thick sample. After deposition, the films were annealed in Argon environment for nearly two hours, cooling the films slowly to room temperature.

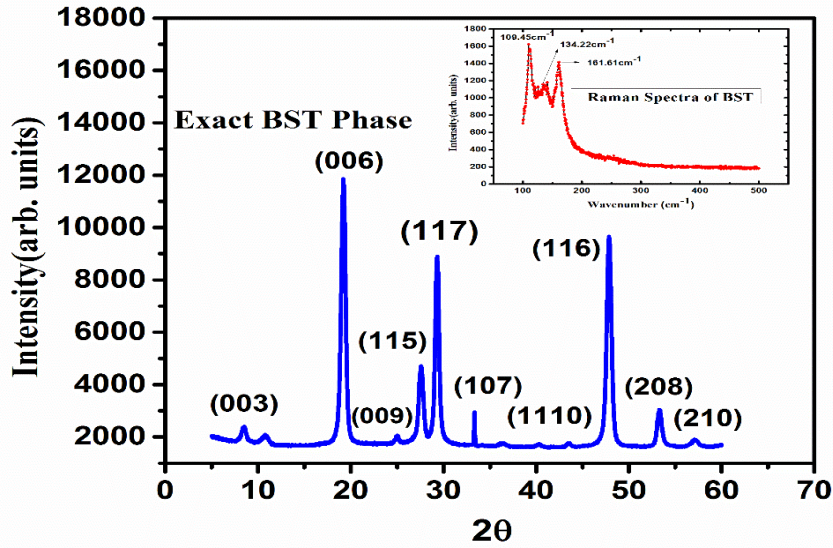


Fig. 1 XRD pattern of BST thin film. Raman spectrum is shown in the inset.

The BST thin films were characterized by X-ray diffraction and Raman spectroscopy as shown in Fig.1. From the XRD analysis it is clear that thin films are in ordered rhombohedral phase of BST and hence are crystalline in nature. Three characteristic Raman peaks have been identified at the position 109.45 cm<sup>-1</sup>, 134.22 cm<sup>-1</sup> and 161.61 cm<sup>-1</sup>. These peaks correspond to the doubly degenerate Raman modes E<sub>2g</sub> and A<sub>2g</sub><sup>2</sup> respectively which are characteristic of the BST sample as previously reported<sup>31</sup>.

### **Results and Discussion**

Transport measurements on thin films were carried out in a cryogen free magnet (Cryogenic, U.K.) in the temperature range of 1.6K to 300K and a maximum magnetic field of 8 Tesla. Before placing

the sample inside the cryogenic system a Hall bar pattern was fabricated using optical lithography technique.

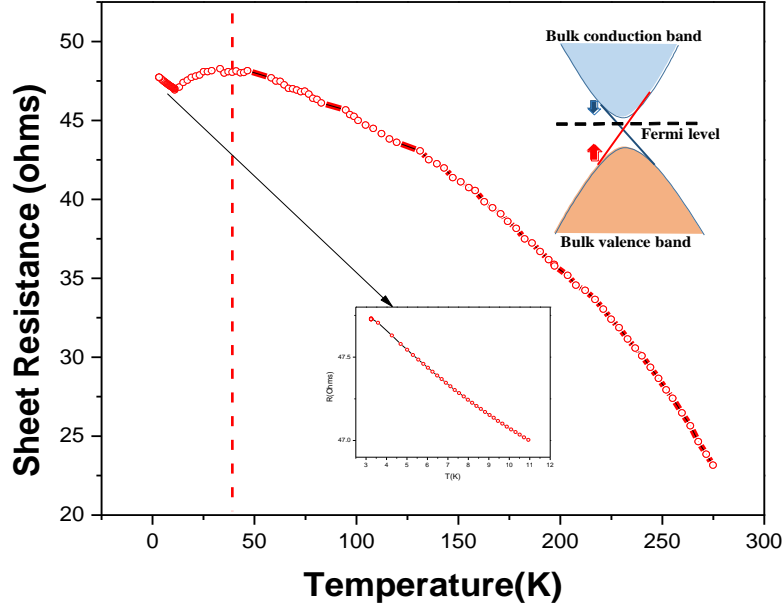


Fig. 2. Resistance variation with temperature. The figure depicts the insulating behavior of BST thin films down to 50K and thereafter it shows insulator to metal transition due to onset of Weak antilocalization (WAL) which dominates over other scattering mechanisms, such as electron – phonon and electron - electron scattering. The dashed vertical line delineates WAL regime from bulk insulating regime. The inset shows an upturn in resistance with decreasing temperature below 10K which is an indication of dominant electron – electron interaction over WAL.

From the Resistance vs. Temperature (R-T) plot in Fig. 2, one can see that the BST thin films show insulating character from room temperature down to 50K. It is quite clear from this plot that the deposited BST sample is in the topological transport regime (below 50K). A crucial requirement for TI is an insulating bulk and surface metallic behavior i.e., the chemical potential should lie in the bulk band gap, intersecting just the Dirac dispersion cones. From the R – T data plot it can be inferred that our sample fulfills this condition. This is in stark contrast to other second generation TI samples such as BS & BT, which display metallic character owing to large number of defect generated bulk carriers<sup>29</sup>. At lower temperatures (fig.2), the bulk states start to localize while surface Dirac states remain delocalized owing to spin momentum locking ( $Z_2$  protection) and possession of a  $\pi$  Berry phase. Similar behavior has been observed in BTS and BST single crystals and other differently doped samples earlier but thin films of these ternary chalcogenides have rarely been studied<sup>14,16,28,36</sup>. This behavior along with low temperature insulator to surface metallic transition ensures ordered occupancy of Se/Te in the quintuple layer unit, which is consistent with

the characteristic XRD peaks of ordered crystal structure of BST thin film. To confirm the insulating nature we had taken the data in both heating and cooling mode but the nature of R-T remained the same which is consistent with other reports<sup>16</sup>. The novel features of the robust Dirac electrons are masked by the notorious trivial electrons in the bulk. The topological Transport regime ensures that the contribution from bulk electrons in the transport measurements are kept to a minimum.

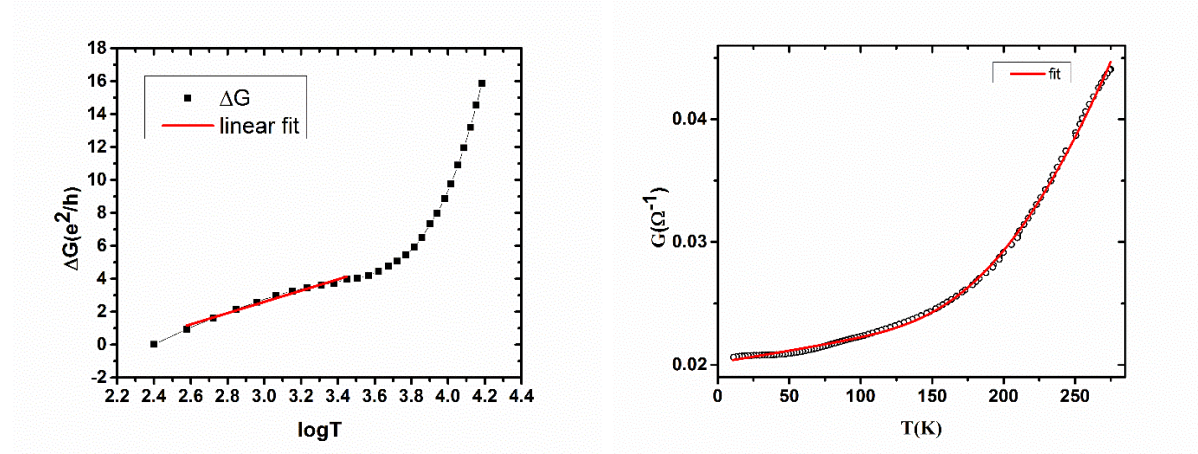


Fig. 3 (a) Plot of change in conductance [where  $\Delta G$  is defined as  $G(10K) - G(50K)$ ] vs.  $\log(T)$  fitted to a linear curve given in equation (1), from 50K down to 10K against  $\log(T)$ . From the trend of the linear fit, it can be inferred that the sample exhibits WAL induced conductance correction behavior below 50K which is in contrast to the conventional weak localization theory for two dimensional electron systems. (b) Conductance data fitted to a non-linear curve which includes both surface and bulk contribution to the conductance.

Interesting features of the electron transport can be inferred from the temperature dependence of resistance (fig.2), especially in the low temperature regime. The existence of WAL depends on the competition between the phase coherence of the electron wave function and the dephasing factors present in the system. Temperature plays a crucial role in this dephasing mechanism. With lowering temperature as the phonon contribution reduces in the system, a pronounced WAL type behavior can be seen in the R-T data. Therefore, temperature dependent WAL behavior below 50K can be represented by the following equation:

$$\delta G = (e^2/h)c \ln T ;$$

$$\text{or } \Delta R_{\square}(T)/R_{\square}(T_0) = -\alpha p (e^2/2\pi\hbar^2) R_{\square} \ln(T/T_0) \quad - \quad (1)$$

Here  $c$  is a constant with value  $c = 1/\pi$ , which is characteristic for two dimensional decoupled surface conduction. From the fit the extracted value of  $c$  is found to be 3. This equation physically describes the WAL induced reduction in the resistance which is consistent with recent theoretical

reports<sup>45</sup>. Thus, from the lowering of the resistance in the R-T profile (fig.2) we can infer the onset of WAL.

Parallel channel conductance model has been used to fit the conductance vs T plot as shown in Fig. 3(b). The two parallel channels being bulk conductance ( $G_b$ ) and surface conductance ( $G_s$ ). The combination of bulk and surface conductance, total conductance;  $G_t$  is represented by:

$$\begin{aligned} G_t &= G_b + G_s \\ &= 1 / (Re^{\Delta/T}) + 1 / (A+BT) \end{aligned} \quad - (2)$$

$G_b(T) = 1/(Re^{\Delta/T})$  and  $G_s(T) = 1/(A+BT)$ , where  $\Delta$  represents the bulk band gap, the

coefficient  $A$  stands for disorder scattering which is independent of temperature, and  $B$  represents electron phonon scattering<sup>46</sup>. At high temperatures, conductance is dominated by the thermal activation of the bulk channel. But as the temperature is reduced a freezing out of bulk carriers take place and surface conductance dominates the proceedings.

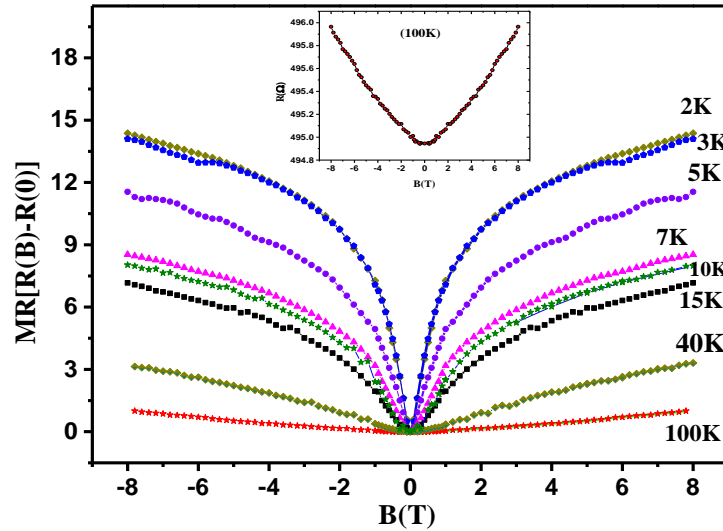


Fig. 4. Magnetoresistance (MR) measured at different temperatures starting from 2K to 100K. A sharp rise in MR around zero field (WAL) at lower temperatures is clearly comprehended from the above plot. The MR at 100K is shown in the inset which exhibits robust nature of surface Dirac states, but it is not characteristic WAL (sharp logarithmic dip in MR) rather it is combined response of activated carriers ( $B^2$  dependence) and metallic surface states, consistent with the R-T in fig2. The parabolic MR is followed by linear MR in the high field regime.



Observation of various quantum interference phenomena in TI has been one of the important tools to characterize the backscattering immune topological surface states. In systems with large spin orbit interaction, having an odd number of Dirac cones the electron wave function gathers a “ $\pi$ ” Berry phase as it circulates along a closed path on the iso-energetic Fermi circles in a Dirac cone. This results in destructive interference between two time reversed coherent paths of electron waves in a diffusive medium, effectively increasing the probability amplitude for forward scattering, thereby reducing the same for backscattering to almost zero<sup>10,17,18</sup>. These quantum interference phenomena manifest itself in lowering the resistance or making positive quantum correction to the conductivity at low temperatures in zero field (as shown in the R-T plot below 50K). This phenomenon is known as weak antilocalization as opposed to its counterpart weak localization.

From the resistance vs. temperature plot (fig. 2.) we can infer the existence of topological transport regime in the BST samples. This can be understood from the fact that the resistance shows an insulating behavior from room temperature down to 50K and thereafter the resistance falls with decreasing temperature. This feature can be attributed to the dominance of 2D Dirac surface state mediated WAL effect over electron-phonon mediated electron scattering. The dominance of 2D WAL effect below certain temperature is an important observation in the bulk insulating TI's, where the contribution from bulk electrons and electron-phonon (e-p) interaction is absent. Below this critical temperature (50K), e-p interaction starts to weaken and bulk electron freeze out, Dirac fermions face lesser scattering and bulk coupling. As a result Dirac electrons surmount impurities/disorder more easily effectively increasing the conductivity or making the system less dissipative, as we go down to lower temperatures. Therefore one can observe the WAL (intrinsic property of TI's) in the bulk insulating TI samples qualitatively by the nature of the R-T curve itself. We can draw an important conclusion from this observation that the fall in resistance in the R-T curve illustrates the 2D WAL effect. Therefore, for samples in which the contribution of bulk in total conductance is lesser the downturn in resistance will be seen at even higher temperatures. This observation is consistent with the previous reports on BTS, BSTS and other intermediate intrinsic TI candidates<sup>21,35,47</sup>. On the other hand this behavior further provides the proof for the weak e-p coupling between surface Dirac states and the bulk phonons<sup>48</sup>. In bulk insulating TI's decoupled nature of the Dirac states from the bulk phonons can be seen in the down turn in the resistance in the R-T profile<sup>28,30,36,47,49</sup>. In a recent experimental observation of half integer quantum Hall Effect (per surface) in BSTS samples of different thicknesses this down turn has been observed even up to 170K<sup>12</sup>. As thickness decreases the downturn temperature of sheet resistance increases which is a direct manifestation of weak coupling of Dirac electrons with bulk phonons.

WAL in the TI thin films can also be probed by breaking the time reversal symmetry of Dirac electrons by the application of perpendicular magnetic field (B). It must be noted here that bare possession of  $\pi$  Berry phase by the surface Dirac states does not guarantee immunity to the disorder. Graphene possesses  $\pi$  Berry phase but exhibits WAL (positive MR) in a very short range of field and eventually localizes in the high field regime (negative MR). In contrast TI's exhibit a remarkable robustness to the applied field and does not show any negative MR even up to the very high field regime (60T)<sup>50</sup>. This is attributed to the combined topological protection of the Dirac



states ( $Z_2$  protection along with  $\pi$  Berry phase) provided by their bulk band topology and single Dirac cone. Graphene consists of even number of Dirac cones in the first Brillouin zone. Therefore in graphene electrons are localized due to inter-valley or intra-valley scattering, while in TI a single Dirac cone does not support these scattering processes due to absence of backscattering channels or valleys<sup>51,52</sup>. Therefore it is the topological distinction of the bulk band structure between TI's and graphene which separates both the materials in response towards application of field. It may be a possible reason for the non-saturating MR experimentally observed in TI thin films/devices.

A typical MR depicting WAL is shown in the Fig. 4 showing sharp increase in MR in the vicinity of zero field, a characteristic feature of WAL at lower temperatures below 50K. As temperature is increased from the lowest temperature the cusp like feature near zero field in MR starts to weaken and eventually disappears above 40K. This is mainly due to the fact that contribution from the bulk carriers and impurity states start increasing and MR exhibits a mixed response from surface as well as bulk states, which is consistent with the R-T behavior in fig.2. Therefore a combination of cusp like feature from Dirac states and parabolic MR ( $MR \propto B^2$ ) from the bulk states appears in the form of linear like field dependence and it extends up to 100K (see inset of fig.4). The fact that quantum coherence in these thin films persisting up to relatively high temperatures suggests and further proves that the major contribution in the conduction is from 2D Dirac fermions. These observations sharper cusp in MR at low temperature and response of Dirac fermions at higher temperatures say 100K combined with the insulating R-T profile together make ternary TI's better than the previous binary ones, which are metallic and do not have high temperature quantum phase coherence<sup>14,31,53–56</sup> Earlier in the experiments on metallic TI thin films, utilizing tuning of chemical potential by electrostatic gating in the bulk band gap (intersecting Dirac cone only, near to Dirac point) it has been observed that slope of weak field MR, and amplitude of quantum oscillations at higher fields, increases quite remarkably. This is a direct consequence of the dominated quantum interference mediated by 2D Dirac fermions at a 2D Fermi surface. Moreover it was found that the phase coherence length and mobility (mean free path) also increased significantly, a distinct signature of robustness of Dirac states. Similarly by growing bulk insulating TI thin films, these features have been observed in comparison to the metallic TI nanostructures.

From the temperature dependence of WAL it is clear it persists even at higher temperatures (100K), though reduced, showing a remarkable robustness of the surface Dirac states towards electron-phonon interaction. This can only be attributed to the bulk insulating nature of these thin films. Low field nature of the 100K MR is the mixture of the classical ( $MR \propto B^2$ ) and WAL induced MR. However, the classical MR dominates therefore it looks like parabolic in nature. In high field regime MR becomes almost linear and the possible reason for its origin is unknown and debatable. But some reports attribute linear response of MR to the surface states but at such a high temperature there can be sufficient electron-phonon interactions which may override the surface Dirac state contribution to conduction. However on the basis of some ARPES studies it has been found that surface Dirac states are very weakly coupled to the bulk phonon bath beneath, therefore we can attribute it to the mixed phase of MR arising from classical as well as quantum effects. From the temperature dependent resistivity in fig.2 we observe that the bulk contribution to the resistance

keeps on decreasing with decreasing temperature in the temperature range of 50K-300K. The sample is in an effective two parallel conducting channel mode. An admixture of activated bulk and metallic surface channel contributes to the total conductivity of the system. Therefore we can expect sufficient bulk contribution at these temperatures which is responsible for the quadratic nature of MR at 100K.

In presence of strong spin-orbit interaction, quantum correction to the conductivity in a two dimensional system can be described by Hikami, Larkin and Nagaoka (HLN) formula<sup>57</sup>. This expression is applicable in the diffusive quantum transport regime with low mobility such as thin films deposited by PLD. The HLN equation can be written in the simplified form for the following condition:  $\tau_{so} < \tau_e < \tau_\phi$ , where  $\tau_{so}$ ,  $\tau_e$  and  $\tau_\phi$  are the characteristic time scales corresponding to the spin-orbit scattering, elastic scattering and inelastic scattering of charge carriers. Conductance correction due to WAL is given as:

$$\delta G_{WAL}(B) \equiv G(B) - G(0) \cong \alpha \frac{e^2}{2\pi^2 \hbar} \left[ \Psi\left(\frac{1}{2} + \frac{B_\phi}{B}\right) - \ln\left(\frac{B_\phi}{B}\right) \right] \text{-----} (3)$$

Where  $\Psi$  is digamma function and  $B_\phi = \hbar / 4el\phi^2$  is characteristic magnetic field corresponding to the coherence length  $l_\phi$ . The value of coefficient “ $\alpha$ ” signifies effective number of coherent channels contributing to conduction and is related to the dimensionality of the metallic state in system. For TI thin films the value of transport coefficient should be equal to 1 corresponding to two surfaces (the top and bottom surface) , but experimentally this value has been found to vary from 0.4 to 1.1, depending on the different conditions such as type of the sample (metallic or bulk insulating ones) or the type of electrostatic gating<sup>22,53,55,58–63</sup> resulting in decoupling of the two conducting channels.

Fitting of magneto-conductance by HLN equation (3) in the low field regime at different temperatures is shown in the Fig. 5(a) and the extracted parameters “ $\alpha$ ” and phase coherence length “ $l_\phi$ ” are plotted as a function of temperature in Fig. 5(b). In the bulk insulating and decoupled regime we have observed strong robustness of the conduction channel parameter “ $\alpha$ ” which hovers around “0.5”. This points towards a single channel coherent transport. In such a situation it is very important to identify the dominant mechanism responsible for the robustness of the value of  $\alpha$ . The parameters which decide whether there is any surface to bulk coupling are  $\tau_{sb}$  and  $\tau_\phi$ , where  $\tau_{sb}$  is the effective surface to bulk scattering time and  $\tau_\phi$  is the phase coherence time. As long as  $\tau_{sb}$  is greater than  $\tau_\phi$ , the bulk and surface serve as two independent channels since the carriers lose their coherence before they scatter into the bulk. But in the opposite scenario when the phase coherence time dominates over surface to bulk scattering time, the carriers maintain their coherence. This results in bulk and surface states behaving as if they possess an effective single phase coherent channel which we observe in previous metallic thin films<sup>31</sup>. In these films it is evident that the

surface to bulk scattering time  $\tau_{sb}$  is very large compared to the phase breaking time  $\tau_\phi$  of surface Dirac fermions on these films of thickness larger than 10nm, i.e.,  $\tau_\phi \ll \tau_{sb}$ , therefore there is no possibility for a surface to bulk coherent transport in such a situation as seen by insulating R-T behavior (fig2.). We can certainly state here that there is a decoupled transport and negligible contribution from the bulk in the fitted temperature range<sup>62</sup>.

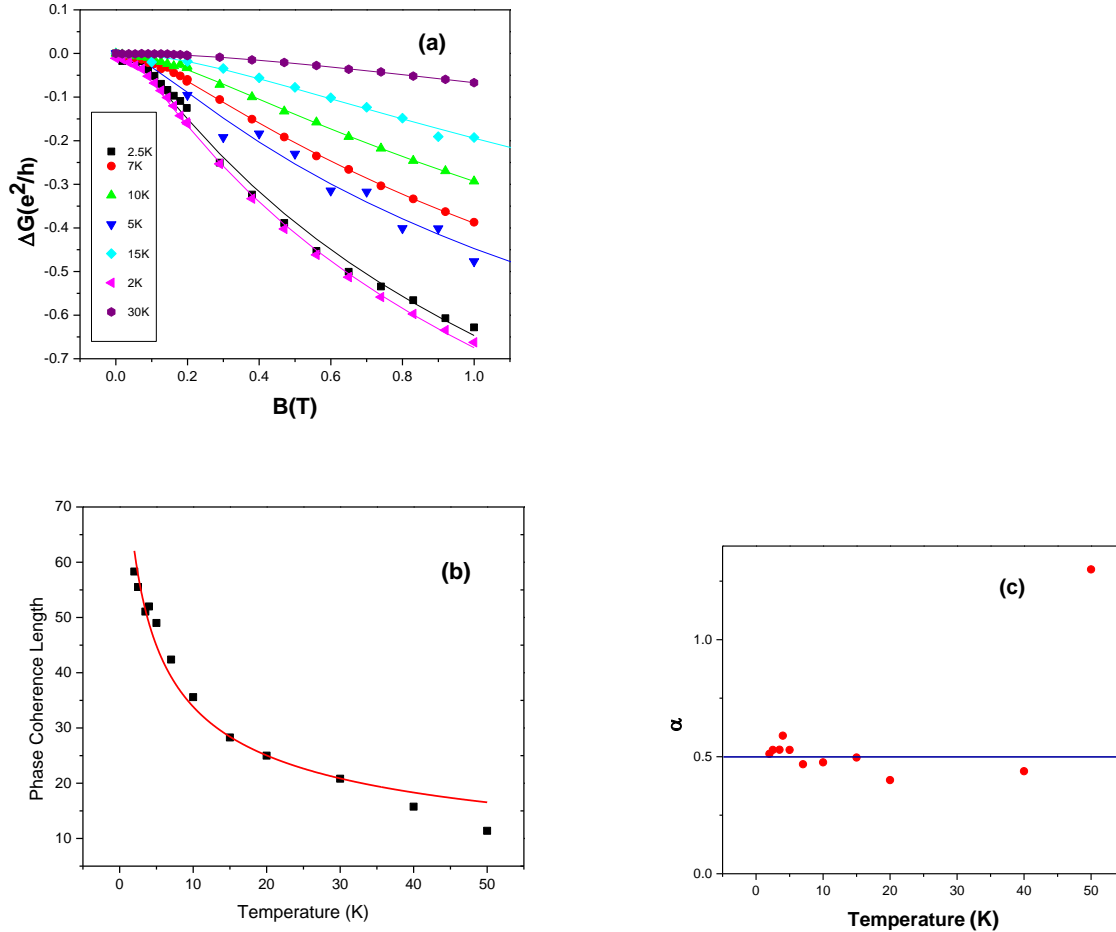


Fig. 5(a) HLN fit of conductance data at different temperatures. (b) Phase coherence length as a function of temperature fitted with power law from the fit we get:  $l_\phi = T^{-0.466}$  which indicates 2D transport in the sample which is consistent with the R-T behavior in fig.2. (c) Variation of  $\alpha$  with temperature. Above 40K there is mixed conduction of surface states and bulk states, therefore value of transport coefficient  $\alpha$  deviates from the 2D values, which again supports the explanation of 2D WAL induced downturn (fig.2) in sheet resistance below 50K.

From the magnetoconductance (MC/MR) analysis of these devices by 2D single channel Hikami Larkin and Nagaoka Model we have observed that the coefficient “ $\alpha$ ” shows remarkable robustness in the temperature range 2K – 40K. The values of coefficient “ $\alpha$ ” obtained by fitting the change in MC( $\Delta G$ ) vs.  $B$  data to the HLN model yielding around 0.5 signifies the presence of

only one channel. Phase coherence length on the other hand decreases monotonically with increasing temperature which is justified. This is because, as the temperature of the system is increased phonons start creeping into the system. These phonons play a pivotal role in the dephasing mechanism and thus reduce the phase coherence length. The thickness of these devices are 200nm and 300nm, where there is no chance of coherent coupling to the bulk charge carriers, since coherence length extracted at these temperatures are far too less (58nm) than the thickness of the devices. Moreover temperature dependent resistivity measurement suggests that no or negligible bulk state contribution exists at these temperatures providing further evidence of no surface to bulk coupling. The value of  $\alpha$  signifies the number of conduction channels contributing to the conduction in a strongly spin orbit coupled two dimensional system. The value of  $\alpha$  for TI thin films and devices extracted from the HLN model have been reported to vary between 0.3 – 1.5 and there is no general consensus among the various reported works. Thus a further modification in the exact model is required which describes topological behavior of TI transport and throws new light in this direction. Nevertheless HLN model, in spite of the fact it incorporates random spin orbit interaction in parabolic bands ( $E \propto k^2$  and not  $E \propto k$  as expected for Dirac Fermions), captures almost all the features of the topological transport. The extracted parameters obtained from fitting of the MR data have shown remarkable consistency with other observations, depending on different physical conditions of TI samples.

Earlier studies based on the two channel conduction in TI thin films and nano devices in ultrathin and thick limit have shown that the value of the coefficient “ $\alpha$ ” depends on various parameters such as gating voltage, compensation doping, intrinsic alloy solutions and thickness of the films or nano device at a particular temperature<sup>22,64,65</sup>. However in principle, for a sample in topological transport regime having two decoupled surface channels, the value of  $\alpha$  should not depend on the aforesaid mentioned parameters. Experimentally there is no general consensus among the various reported values of  $\alpha$  for TI thin films.<sup>22,59–61,64–66</sup>. But for thick films, “ $\alpha$ ” is not expected to change with ‘T’. That is why we considered a thick film to see the effect of various parameters on “ $\alpha$ ”.

There are reports indicating that the bulk states and quantum confined surface states in TI start localizing at around the same time when the Dirac surface states become more dominating with decreasing temperature, owing to the reduced electron phonon scattering and spin momentum locking ( $\pi$  Berry phase)<sup>44,60,61,67–69</sup>. One can clearly see this demarcation between the two regimes from the R – T plot, where the dotted line in Fig. 2 separates the two regimes. Since bulk states are randomly oriented, on an average they do not exhibit WAL, while the trivial 2D surface states coexisting with surface Dirac fermions do not have topological protection and hence are not immune to the localization coming from disorder potential. These bulk and 2DEG state’s combined contribution may give rise to a weak localization correction component to the conductivity at low temperatures and hence an effective positive contribution to the effective total value “ $\alpha_T$ ” making it close to 0.5 as observed from the fitting to the HLN equation in Fig. 5(b)<sup>10,60</sup>.

The phase coherence length ( $l_\phi$ ) extracted from the fit does not show any improvement as is expected to be the case with the ternary tetradymites, with high bulk insulating TI candidates. As reflected in the R – T graph this sample exhibits insulating nature, underlying the fact that the Fermi level lies in the bulk gap (topological transport regime). One possible explanation for this

type of behavior can be attributed to the coexistence of the 2DEG on the surface participating in the 2D electron conduction along with the non-trivial Dirac fermions<sup>67,68</sup>. This two dimensional electron gas (2DEG) is formed at the surface of TI's as a result of electron doping when TI samples are exposed to the external environment<sup>67,68</sup>. Formation of this 2DEG results in downward bending of bands near surface making a potential gradient which is asymmetric in nature hence it is of Rashba type. This trivial 2DEG is confined in this triangular like potential and forms separate parabolic bands coexisting with nontrivial topological states, which may split if confinement is stronger or exposure to the external environment is larger. This is captured schematically in fig. 7(a). This 2DEG could be localized completely at low temperatures by the disorder and grain boundaries present in PLD grown thin films. In our thin films there is a high possibility of this downward band bending induced 2DEG, owing to the exposure of external environment while making contacts before inserting samples in the measurement chamber.

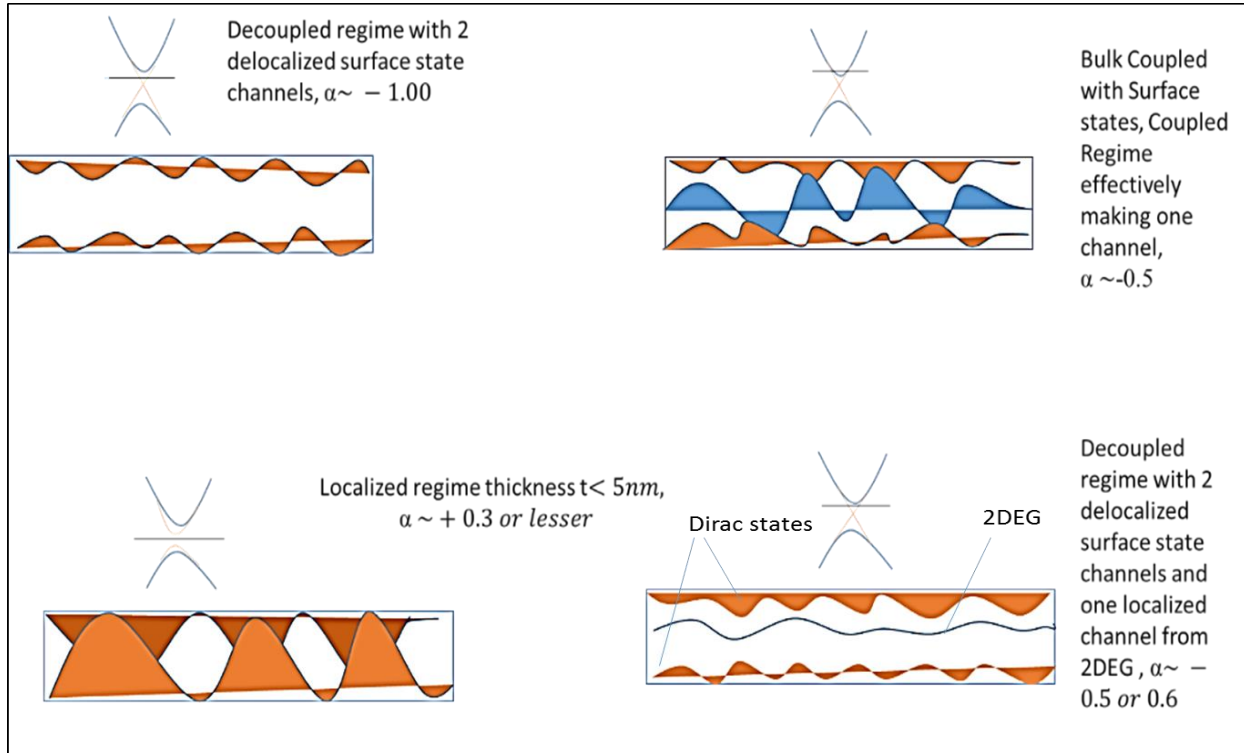


**Fig.6** Schematic explanation of coupled and decoupled transport of surface states in different regime. (a) decoupled transport of by two surface channels in bulk insulating sample providing value of coefficient  $\alpha = (-1/2) + (-1/2) = -1$ . (b) Metallic thin films where bulk and surface channels are coherently coupled and effectively make one channel  $\alpha = -1/2$ . (c) Strongly localized regime when thickness of the film is below critical thickness  $t < 5\text{nm}$ . (d) Decoupled transport in a bulk insulating film when exposed to the external environment. Due to the downward band bending a trivial 2DEG

is formed beneath the upper surface. Apart from delocalized Dirac fermions on two surfaces this confined 2DEG gets localized at low temperature and the value of  $\alpha$  is the result of mixed contribution from localization and antilocalization phenomena. It should be noted that we did not include the hexagonal warping effect, which is responsible for finite backscattering of Dirac fermions since chemical potential on the top surface is near the conduction band edge. Far away from the Dirac point there is a finite warping of the Dirac cone due to crystal potential which develops out of plane spin component which enhances the probability for backscattering (see ref.32 and 33).

We deposited thick films followed by annealing in the Argon environment for 2hrs in order to decouple the two surfaces and as a result we should have got the value of  $\alpha$  around 1 – 1.15 as reported in some of the earlier works on thin films and single crystals. But the robustness of the value of  $\alpha$  (0.5 – 0.6) with increasing temperature as extracted from the fitting of HLN equation has raised further questions. This is especially due to the fact that in our R vs. T plot (Fig.2) we clearly see a decoupled surface and bulk transport below 50 K. The only possible explanation for these values of  $\alpha$  in decoupled regime can be competitive nature of WAL and WL originating from surface Dirac states and trivial quantum confined states respectively. For two surface states, WAL yields value of the coefficient  $\alpha$  (which is negative and nearly ‘-1’ for capped TI thin films or unexposed to ambient atmosphere) and a positive value of  $\alpha$  (say 0.4 - 0.3) coming from the localization of the nontrivial 2DEG and bulk impurity states, which comes in to play due to band bending/Rashba splitting arising from environmental exposure. Therefore, the resultant effect of these two phenomena results in the coefficient  $\alpha$  to be -0.5. Quantitatively it can be expressed in the form of an equation.

$$\alpha_T = \alpha [\text{WAL (-ve)}] + \alpha [\text{WL (+ve)}] \approx 0.5 - 0.6$$

$$\alpha = f(\tau_\phi/\tau_{SB}) + f(\text{disorder or 2D quantum confined gas})$$

Surface reconstruction processes arising due to aging of sample in the external environment leads to downward band bending near the top surface of TI thin films, forming accumulation layers of quantum confined 2DEG<sup>67,68</sup>. This results in quantum confined states due to asymmetric potential as illustrated schematically in the Fig.7 below. Therefore, we believe there are three channels in these TI thin films, two conducting surface Dirac channels belonging to top and bottom surfaces and third one originating from trivial 2DEG which is quantum confined and is present only at the top surface. The Dirac fermion channels are topologically delocalized hence exhibit WAL while 2DEG shows localization behavior as one goes down in temperature. If a passivating layer is applied on these TI films, we believe we can get rid of the surface degradation induced 2D quantum confined electron gas on the top surface while bottom surface remains protected. Therefore according to the ARPES reports chemical potential of the top surface of our TI thin films crosses the Rashba split 2D sub-bands while that of bottom surface remains between the Dirac point and

conduction band edge (upper Dirac cone). In this condition we can get the value of transport coefficient  $\alpha = 1$ , if transport is decoupled by the bulk insulating nature of TI thin film.<sup>8,44</sup>

WAL in 2D Rashba split quantum well states is observed in the ballistic regime. The system is said to be in the ballistic regime when  $k_f l_e \gg 1$  or  $k_B T \tau / \hbar \gg 1$ , mobility  $\mu = 8000 - 20000 \text{ cm}^2/\text{Vs}$  or more (here  $k_f$  is fermi wave vector,  $l_e$  is mean free path,  $k_B$  Boltzmann constant,  $\hbar$  reduced plank coefficient,  $\tau$  is transport life time and  $T$  is the temperature in kelvin). One should have extremely low temperatures (mK range) to observe WAL in these 2DEG systems and at slightly high temperatures the WAL cusp in MR vanishes. Moreover magnitude of the WAL (change in the resistance in presence of field) is very less as compared to the case of surface Dirac states. These requirements to flip electron spin from random orientation by Rashba spin orbit interaction pose serious questions about the WAL behavior of 2DEG in heavily disordered systems<sup>70</sup> (mobility  $\mu = 20 - 30 \text{ cm}^2/\text{Vs}$ ). This is true at least in our case of polycrystalline thin films having larger grains which is evident from SEM data. The simultaneous observation of the clearly resolved beating pattern of SdH oscillations along with less sharp cusp of WAL (in the low field regime) in other 2D Rashba split systems allow us to conclude that in case of PLD deposited TI thin films 2DEG will rather exhibit some amount of localization due to low mobility (larger disorder).

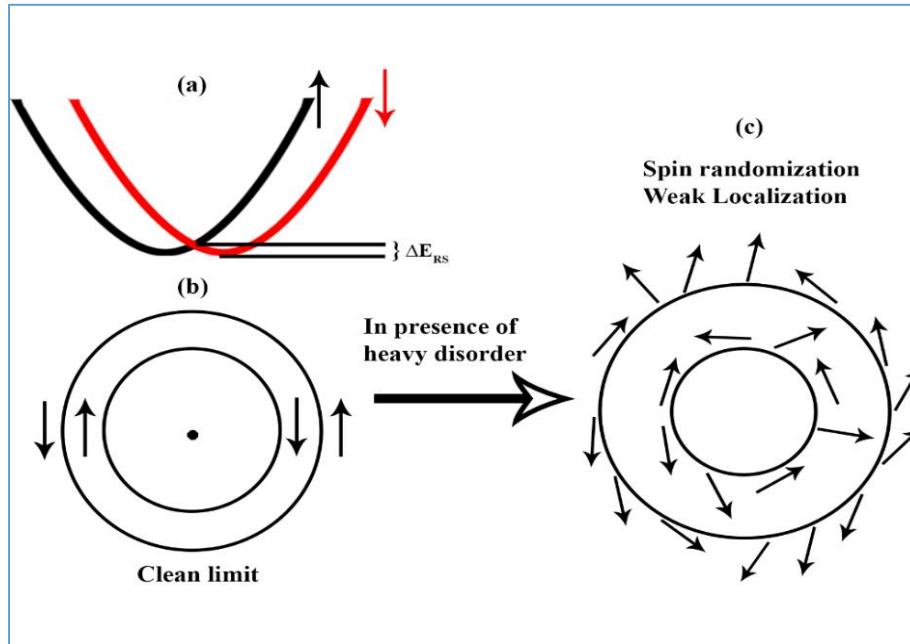


Fig. 7. (a) Rashba split bulk 2D sub-bands in TI due to formation of the quantum confined states at the top surface of thin film. The arrows indicate spin direction of the electronic states. (b) Energy contour of these states and the channels for the inter-valley scattering in the clean limit (very high mobility). (c) Effect of the disorder on the spin orientation on these states exhibiting complete spin randomization, which suppresses WAL coming out of spin split 2DEG effectively. Note that the bulk conduction band and valence bands have not been shown in the figure. The sub-band states shown here are just below the bulk conduction band.



WAL and SdH oscillations both show response to only perpendicular component of the magnetic field however there are some reports where SdH oscillations have shown contribution from the bulk as well<sup>71</sup>. In case of sample surface degradation even by an hour exposure to ambient atmosphere, these quantum oscillations disappear but WAL on the other hand is remarkably robust even in samples exposed for many days. Hence we can claim that WAL, in bulk insulating samples is considerably reliable and a better tool to probe the TI surface states in comparison to SdH oscillations. Moreover to observe quantum oscillations in the samples of TI one needs to fulfill the condition;  $\mu B \gg 1$  which require very high quality samples with high mobility and high B field. On the other hand WAL is a low field phenomena and is observed in the range of 0- 1 Tesla. WAL can be seen even in samples with very low carrier mobility (diffusive regime, i.e.,  $\mu B \ll 1$ ). PLD deposited films, are a lot more cost effective than single crystals.

Our argument is based on the idea that in PLD grown samples one cannot avoid the exposure from the external environment. Hence there is a surface degradation due to formation of the trivial 2DEG owing to the quantum confinement effects (downward band bending in our case because of n type carriers)<sup>64,67</sup>. This in turn results in enhancement of surface carrier density (as large as 40%). These trivial states are topologically unprotected and vulnerable to localization in the presence of disorder and grain boundaries (very low mobility). Their contribution to WAL is very feeble but by the same measure one cannot have quantum oscillations. Moreover the mobility and surface carrier density extracted by SdH analysis do not provide the Dirac fermionic nature and robustness of TI surface states (underestimated values). This in turn results in miscalculated value of mobility ' $\mu$ ' of the sample and erroneous value of surface Dirac carrier density which coexist with trivial 2DEG. Moreover extracted multiple SdH frequencies or single frequency make the physical interpretation of possible fermi surfaces and their origin very complex and challenging apart from few reports<sup>9,49,72</sup>.

In some reports,<sup>73</sup> it has been argued that quantum confined two dimensional electron states take part in WAL owing to the Rashba spin splitting, but these trivial 2DEG states may exhibit WAL only in low field regime (<100 mT) in comparison to the WAL exhibited by topologically protected Dirac states in (intermediate field regime Tesla) which is three order of magnitude larger than the former. 2DEG localizes in low field regime (<100 mT) showing a maximum in MR, thereafter followed by a negative MR exhibiting an M like curve. But it has been observed in TI thin films that the sharp cusp like feature in MR lasts up to a high magnetic field range of several Tesla and followed by linear MR or quantum oscillations depending on the quality of sample or strength of the applied external field. The magnitude of WAL cusp induced by topologically protected Dirac states is very large compared to that of the trivial 2DEG so that it hardly affects the magnitude of WAL cusp (TI states). Therefore, contribution to the quantum correction to the conductivity from 2DEG is mainly from the localization channel of it. Moreover, the magnitude of Rashba splitting of quantum well states in TI thin films depends upon the time of the exposure and the type of the exposure which determine the nature of conduction, but the Rashba splitting energy in TI thin films exposed for a limited time has been found experimentally very weak. In such a case we could expect mainly weak localization contribution of 2DEG<sup>62</sup>. Taskin and N.

Bansal et al have shown in their study on the formation of quantum well states and their effect on the surface conduction<sup>8,44</sup>. In their study the value of transport coefficient “ $\alpha$ ” on the TI thin films of different thicknesses support our findings. Therefore, we can conclude from these arguments that the contribution of 2DEG to the transport coefficient “ $\alpha$ ” is only positive corresponding to the localization. In some recent studies on decoupled bulk insulating TI samples the upper surface is passivated. This passivation shields the upper surface from degradation and formation of any such 2DEG states. For such a system both bottom and upper surface contribute equally to give coefficient  $\alpha$  value 1. These reports thus support our findings and strengthen our physical explanation on the deviation of  $\alpha$  and  $l_\phi$  from its ideal values.

## Conclusion:

In this study our main focus was to optimize the BST samples in topological transport regime where bulk has negligible or very little significance in terms of contribution to transport as it is clearly manifested in the  $R - T$  plot. Secondly, we have prepared very thick films to decouple the two surface states with the bulk where condition  $\tau_\phi/\tau_{sb} \ll 1$  is satisfied so that we could investigate the value of the transport channel coefficient “ $\alpha$ ” which in principle must be 1 for these samples. A coherent and comprehensive understanding has been given for the different values of the transport coefficient “ $\alpha$ ” based on experimental conditions and sample properties. It is remarkable feature that PLD grown thin films which are highly insulating in the bulk and thereby residing in the topological transport regime. PLD is a better deposition technique as compared to other synthesis techniques in terms of cost and time consumption to make a thin film. Annealing of the thin films in slightly elevated temperature makes the selenium atoms occupy ordered states between central layers of the Quintuple Layers. Thus annealing not only reduces the defects in the TI thin films but improves the surface morphology and smoothness, crystallinity and grain structure. In contrast to the restriction of observation of Quantum Oscillation only at very low temperature regime (due to thermal smearing of the cyclotron orbits) WAL is robust at higher temperatures exhibiting quantum coherence up to 100K, which makes it superior to SdH oscillations.

## References

1. Ando, Y. Topological Insulator Materials. *J. Phys. Soc. Japan* **82**, 102001 (2013).
2. Hasan, M. & Kane, C. Colloquium: Topological insulators. *Rev. Mod. Phys.* **82**, 3045–3067 (2010).
3. Qi, X. L. & Zhang, S. C. Topological insulators and superconductors. *Rev. Mod. Phys.* **83**, (2011).
4. Nomura, K., Koshino, M. & Ryu, S. Topological delocalization of two-dimensional massless dirac fermions. *Phys. Rev. Lett.* **99**, (2007).

5. Suzuura, H. & Ando, T. Crossover from symplectic to orthogonal class in a two-dimensional honeycomb lattice. *Phys. Rev. Lett.* **89**, 266603 (2002).
6. Fu, L. & Kane, C. Topological insulators with inversion symmetry. *Phys. Rev. B* **76**, 45302 (2007).
7. Qi, X.-L. & Zhang, S.-C. The quantum spin Hall effect and topological insulators. *Phys. Today* (2010). doi:10.1063/1.3293411
8. Taskin, A. A., Sasaki, S., Segawa, K. & Ando, Y. Manifestation of Topological Protection in Transport Properties of Epitaxial Bi<sub>2</sub>Se<sub>3</sub> Thin Films. *Phys. Rev. Lett.* **109**, 66803 (2012).
9. Xiong, J. *et al.* Quantum oscillations in a topological insulator Bi<sub>2</sub>Te<sub>2</sub>Se with large bulk resistivity (). *Phys. E Low-dimensional Syst. Nanostructures* **44**, 917–920 (2012).
10. He, H.-T. *et al.* Impurity Effect on Weak Antilocalization in the Topological Insulator Bi<sub>2</sub>Te<sub>3</sub>. *Phys. Rev. Lett.* **106**, 4 (2011).
11. Hsieh, D. *et al.* A topological Dirac insulator in a quantum spin Hall phase. *Nature* **452**, 970–974 (2008).
12. Xia, Y. *et al.* Observation of a large-gap topological-insulator class with a single Dirac cone on the surface. *Nat. Phys.* **5**, 398–402 (2009).
13. Wray, L. A. *et al.* A topological insulator surface under strong Coulomb, magnetic and disorder perturbations. *Nat. Phys.* **7**, 32–37 (2010).
14. Ren, Z., Taskin, A. A., Sasaki, S., Segawa, K. & Ando, Y. Large bulk resistivity and surface quantum oscillations in the topological insulator Bi<sub>2</sub>Te<sub>2</sub>Se. *Phys. Rev. B - Condens. Matter Mater. Phys.* **82**, 0–3 (2010).
15. Peng, H. *et al.* Aharonov-Bohm interference in topological insulator nanoribbons. *Nat. Mater.* **9**, 225–229 (2010).
16. Bao, L. *et al.* Weak anti-localization and quantum oscillations of surface states in topological insulator Bi<sub>2</sub>Se<sub>2</sub>Te. *Sci. Rep.* **2**, 726 (2012).
17. Bergmann, G. WEAK LOCALIZATION IN THIN FILMS a time-of-flight experiment with conduction electrons. *Phys. Rep.* 1–58 (1913).
18. Bergmann, G. Physical interpretation of weak localization: A time-of-flight experiment with conduction electrons. *Phys. Rev. B* **28**, 2914–2920 (1983).
19. Mellnik, A. R. *et al.* Spin-transfer torque generated by a topological insulator. *Nature* **511**, 449–451 (2014).

20. Shiomi, Y. *et al.* Spin-Electricity Conversion Induced by Spin Injection into Topological Insulators. *Phys. Rev. Lett.* **113**, 196601 (2014).
21. Xu, Y. *et al.* Observation of topological surface state quantum Hall effect in an intrinsic three-dimensional topological insulator. *Nat. Phys.* **10**, 956–963 (2014).
22. Hong, S. S., Cha, J. J., Kong, D. & Cui, Y. Ultra-low carrier concentration and surface-dominant transport in antimony-doped Bi<sub>2</sub>Se<sub>3</sub> topological insulator nanoribbons. *Nature Communications* **3**, 757 (2012).
23. Miyamoto, K. *et al.* Topological Surface States with Persistent High Spin Polarization across the Dirac Point in Bi<sub>2</sub>Te<sub>2</sub>Se and Bi<sub>2</sub>Se<sub>2</sub>Te. *Phys. Rev. Lett.* **109**, 166802 (2012).
24. He, X. *et al.* Highly tunable electron transport in epitaxial topological insulator (Bi<sub>1-x</sub>Sb<sub>x</sub>)<sub>2</sub>Te<sub>3</sub> thin films. *Appl. Phys. Lett.* **101**, 123111 (2012).
25. Gehring, P., Gao, B., Burghard, M. & Kern, K. Two-dimensional magnetotransport in Bi<sub>2</sub>Te<sub>2</sub>Se nanoplatelets. *Appl. Phys. Lett.* **101**, 23116 (2012).
26. Ren, Z., Taskin, a., Sasaki, S., Segawa, K. & Ando, Y. Optimizing Bi<sub>2-x</sub>Sb<sub>x</sub>Te<sub>3-y</sub>Se<sub>y</sub> solid solutions to approach the intrinsic topological insulator regime. *Phys. Rev. B* **84**, 1–6 (2011).
27. Cheng, P. *et al.* Landau Quantization of Topological Surface States in Bi<sub>2</sub>Se<sub>3</sub>. *Phys. Rev. Lett.* **105**, 76801 (2010).
28. Neupane, M. *et al.* Topological surface states and Dirac point tuning in ternary topological insulators. *Phys. Rev. B* **85**, 235406 (2012).
29. Scanlon, D. O. *et al.* Controlling bulk conductivity in topological insulators: key role of anti-site defects. *Adv. Mater.* **24**, 2154–2158 (2012).
30. Ren, Z., Taskin, A. A., Sasaki, S., Segawa, K. & Ando, Y. Observation of Dirac Holes and Electrons in a Topological Insulator. *Phys. Rev. B* **107**, 1–4 (2011).
31. Gopal, R. K., Singh, S., Chandra, R. & Mitra, C. Weak-antilocalization and surface dominated transport in topological insulator Bi<sub>2</sub>Se<sub>2</sub>Te. *AIP Adv.* **5**, 047111 (2015).
32. Nomura, M. *et al.* Relationship between Fermi surface warping and out-of-plane spin polarization in topological insulators: A view from spin- and angle-resolved photoemission. *Phys. Rev. B* **89**, 45134 (2014).
33. Kuroda, K. *et al.* Hexagonally Deformed Fermi Surface of the 3D Topological Insulator Bi<sub>2</sub>Se<sub>3</sub>. *Phys. Rev. Lett.* **105**, 076802 (2010).

34. Wang, Y. H. *et al.* Observation of a Warped Helical Spin Texture in Bi<sub>2</sub>Se<sub>3</sub> from Circular Dichroism Angle-Resolved Photoemission Spectroscopy. *Phys. Rev. Lett.* **107**, 207602 (2011).
35. Zhang, J. *et al.* Band structure engineering in (Bi<sub>1-x</sub>Sb<sub>x</sub>)<sub>2</sub>Te<sub>3</sub> ternary topological insulators. *Nat. Commun.* **2**, 574 (2011).
36. Arakane, T. *et al.* Tunable Dirac cone in the topological insulator Bi<sub>2-x</sub>Sb<sub>x</sub>Te<sub>3-y</sub>Se<sub>y</sub>. *Nat. Commun.* **3**, 636 (2012).
37. Xu, S.-Y. *et al.* Hedgehog spin texture and Berry's phase tuning in a magnetic topological insulator. *Nat. Phys.* **8**, 616–622 (2012).
38. Souma, S. *et al.* Direct Measurement of the Out-of-Plane Spin Texture in the Dirac-Cone Surface State of a Topological Insulator. *Phys. Rev. Lett.* **106**, 216803 (2011).
39. Kou, X. *et al.* Scale-Invariant Quantum Anomalous Hall Effect in Magnetic Topological Insulators beyond the Two-Dimensional Limit. *Phys. Rev. Lett.* **113**, 137201 (2014).
40. Pesin, D. & MacDonald, A. H. Spintronics and pseudospintronics in graphene and topological insulators. *Nat. Mater.* **11**, 409–16 (2012).
41. Van 't Erve, O. M. J. *et al.* Electrical injection and detection of spin-polarized carriers in silicon in a lateral transport geometry. *Appl. Phys. Lett.* **91**, 212109 (2007).
42. Jedema, F. J., Heersche, H. B., Filip, A. T., Baselmans, J. J. A. & van Wees, B. J. Electrical detection of spin precession in a metallic mesoscopic spin valve. *Nature* **416**, 713–6 (2002).
43. Bansal, N. *et al.* Epitaxial growth of topological insulator Bi<sub>2</sub>Se<sub>3</sub> film on Si(111) with atomically sharp interface. *Thin Solid Films* **520**, 224–229 (2011).
44. Bansal, N., Kim, Y. S., Brahlek, M., Edrey, E. & Oh, S. Thickness-Independent Transport Channels in Topological Insulator Bi<sub>2</sub>Se<sub>3</sub> Thin Films. *Phys. Rev. Lett.* **109**, 116804 (2012).
45. Lu, H.-Z. & Shen, S.-Q. Finite-Temperature Conductivity and Magnetoconductivity of Topological Insulators. *Phys. Rev. Lett.* **112**, 146601 (2014).
46. Gao, B. F., Gehring, P., Burghard, M. & Kern, K. Gate-controlled linear magnetoresistance in thin Bi<sub>2</sub>Se<sub>3</sub> sheets. *Appl. Phys. Lett.* **100**, 212402 (2012).
47. Ren, Z., Taskin, A. A., Sasaki, S., Segawa, K. & Ando, Y. Large bulk resistivity and surface quantum oscillations in the topological insulator Bi<sub>2</sub>Te<sub>2</sub>Se. *Phys. Rev. B* **82**, 241306 (2010).

48. Pan, Z.-H. *et al.* Measurement of an Exceptionally Weak Electron-Phonon Coupling on the Surface of the Topological Insulator Bi<sub>2</sub>Se<sub>3</sub> Using Angle-Resolved Photoemission Spectroscopy. *Phys. Rev. Lett.* **108**, 187001 (2012).
49. Xiong, J. *et al.* High-field Shubnikov–de Haas oscillations in the topological insulator Bi<sub>2</sub>Te<sub>3</sub>. *Phys. Rev. B* **86**, 45314 (2012).
50. Zhang, S. X. *et al.* Magneto-resistance up to 60 Tesla in topological insulator Bi<sub>2</sub>Te<sub>3</sub> thin films. *Appl. Phys. Lett.* **101**, 202403 (2012).
51. Tikhonenko, F. V, Kozikov, A. A., Savchenko, A. K. & Gorbachev, R. V. Transition between Electron Localization and Antilocalization in Graphene. *Phys. Rev. Lett.* **103**, 226801 (2009).
52. Morpurgo, A. F. & Guinea, F. Intervalley Scattering, Long-Range Disorder, and Effective Time-Reversal Symmetry Breaking in Graphene. *Phys. Rev. Lett.* **97**, 196804 (2006).
53. Chen, J. *et al.* Gate-Voltage Control of Chemical Potential and Weak Antilocalization in Bi<sub>2</sub>Se<sub>3</sub>. *Phys. Rev. Lett.* **105**, 1–4 (2010).
54. Kong, D., Koski, K. J., Cha, J. J., Hong, S. S. & Cui, Y. Ambipolar field effect in Sb-doped Bi<sub>2</sub>Se<sub>3</sub> nanoplates by solvothermal synthesis. *Nano Lett.* **13**, 632–636 (2013).
55. Kong, D. *et al.* Ambipolar field effect in the ternary topological insulator (Bi<sub>x</sub>Sb<sub>1-x</sub>)<sub>2</sub>Te<sub>3</sub> by composition tuning. *Nature Nanotechnology* **6**, 705–709 (2011).
56. Ren, Z., Taskin, A. A., Sasaki, S., Segawa, K. & Ando, Y. Optimizing Bi<sub>2-x</sub>Sb<sub>x</sub>Te<sub>3-y</sub>Se<sub>y</sub> solid solutions to approach the intrinsic topological insulator regime. *Phys. Rev. B* **84**, 165311 (2011).
57. Hikami, S., Larkin, A. I. & Nagaoka, Y. Spin-Orbit Interaction and Magnetoresistance in the Two Dimensional Random System. *Prog. Theor. Phys.* **63**, 707–710 (1980).
58. Jauregui, L. A., Pettes, M. T., Rokhinson, L. P., Shi, L. & Chen, Y. P. Gate Tunable Relativistic Mass and Berry's phase in Topological Insulator Nanoribbon Field Effect Devices. 22 (2014). at <<http://arxiv.org/abs/1402.2659>>
59. Lang, M. *et al.* Revelation of topological surface states in Bi<sub>2</sub>Se<sub>3</sub> thin films by in situ Al passivation. *ACS Nano* **6**, 295–302 (2012).
60. Lu, H.-Z. & Shen, S.-Q. Weak localization of bulk channels in topological insulator thin films. *Phys. Rev. B* **84**, 125138 (2011).
61. Cao, H. *et al.* Controlling and distinguishing electronic transport of topological and trivial surface states in a topological insulator. (2014). at <<http://arxiv.org/abs/1409.3217>>

62. Lang, M. *et al.* Competing weak localization and weak antilocalization in ultrathin topological insulators. *Nano Lett.* **13**, 48–53 (2013).
63. Steinberg, H., Gardner, D. R., Lee, Y. S. & Jarillo-Herrero, P. Surface State Transport and Ambipolar Electric Field Effect in Bi(2)Se(3) Nanodevices. *Nano Lett.* 1–4 (2010). doi:10.1021/nl1032183
64. Kim, D., Syers, P., Butch, N. P., Paglione, J. & Fuhrer, M. S. Coherent topological transport on the surface of Bi<sub>2</sub>Se<sub>3</sub>. *Nat. Commun.* **4**, 1–5 (2013).
65. Steinberg, H., Laloë, J.-B., Fatemi, V., Moodera, J. S. & Jarillo-Herrero, P. Electrically tunable surface-to-bulk coherent coupling in topological insulator thin films. *Phys. Rev. B* **84**, 233101 (2011).
66. Garate, I. & Glazman, L. Weak localization and antilocalization in topological insulator thin films with coherent bulk-surface coupling. *Phys. Rev. B* **86**, 35422 (2012).
67. Bianchi, M. *et al.* Coexistence of the topological state and a two-dimensional electron gas on the surface of Bi(2)Se(3). *Nat. Commun.* **1**, 128 (2010).
68. Benia, H. M., Lin, C., Kern, K. & Ast, C. R. Reactive Chemical Doping of the Bi<sub>2</sub>Se<sub>3</sub> Topological Insulator. *Phys. Rev. Lett.* **107**, 177602 (2011).
69. King, P. D. C. *et al.* Large Tunable Rashba Spin Splitting of a Two-Dimensional Electron Gas in Bi<sub>2</sub>Se<sub>3</sub>. *Phys. Rev. Lett.* **107**, 96802 (2011).
70. Miller, J. B. *et al.* Gate-Controlled Spin-Orbit Quantum Interference Effects in Lateral Transport. *Phys. Rev. Lett.* **90**, 76807 (2003).
71. Analytis, J. G. *et al.* Bulk Fermi surface coexistence with Dirac surface state in Bi<sub>2</sub>Se<sub>3</sub>: A comparison of photoemission and Shubnikov-de Haas measurements. *Phys. Rev. B - Condens. Matter Mater. Phys.* **81**, (2010).
72. Taskin, A. A. & Ando, Y. Berry phase of non-ideal Dirac fermions in topological insulators. 2–5 (2011).
73. Lee, J., Lee, J.-H., Park, J., Kim, J. S. & Lee, H.-J. Evidence of Distributed Robust Surface Current Flow in 3D Topological Insulators. *Phys. Rev. X* **4**, 11039 (2014).